



Contents lists available at ScienceDirect

## Journal of King Saud University – Science

journal homepage: [www.sciencedirect.com](http://www.sciencedirect.com)

## Fabrication of shape memory natural rubber using palmitic acid



Jeff Sze-Hua Wee, Ai Bao Chai\*, Jee-Hou Ho

Department of Mechanical, Materials and Manufacturing Engineering, Faculty of Engineering, The University of Nottingham Malaysia Campus, Malaysia

## ARTICLE INFO

## Article history:

Received 12 July 2017

Accepted 8 September 2017

Available online 14 September 2017

## Keywords:

Shape memory

Natural rubber

Swelling

Palmitic acid

## ABSTRACT

This paper investigates the practicability of fabricating a shape memory natural rubber with the use of palmitic acid as the swelling agent. Strips of natural rubber samples were swollen in molten palmitic acid at 75 °C. Equilibrium swelling of natural rubber with palmitic acid was found to occur at approximately 50 min of swelling time. Under cooling effect, the palmitic acid crystallized to form a percolated crystalline platelet network. These networks allow fabricated shape memory natural rubber (SMNR) to deform and recover its shape at a temperature above the melting point of palmitic acid. Under controlled uniaxial stress, the natural rubber sample with 0 parts per hundred rubber (phr) carbon black loading exhibits fixity and recovery of  $80 \pm 10\%$ . Motivation of this research is primarily on practicability of palmitic acid to be used as a swelling agent for shape memory properties. Results show that palmitic acid is a relatively good swelling agent to induce shape memory properties into natural rubber.

© 2017 The Authors. Production and hosting by Elsevier B.V. on behalf of King Saud University. This is an open access article under the CC BY-NC-ND license (<http://creativecommons.org/licenses/by-nc-nd/4.0/>).

## 1. Introduction

Recently, the application of shape memory polymer has been gaining a lot of attention due to its extraordinary dynamic shape memory properties. Shape Memory Polymers (SMP's) are smart materials which can be programmed to a temporary shape until an external stimulus, such as temperature (Luo et al., 2015; Tsukada et al., 2014), light (Lee et al., 2011; Wu et al., 2012), water (Huang et al., 2005) or pH value (Feil et al., 1992) is initiated to activate the shape recovery process to return to their permanent or original shape. Generally, there are at least two different phases in shape memory polymers, which are stable network phase and crystalline phase. The stable phase helps to stabilize and retain the original shape. Deformation of this phase is what drives the shape recovery. This stable phase can be created by introduction of cross-linking chemicals or interpenetrating network (Hu et al., 2012). On the other hand, crystalline phase is responsible in impeding shape recovery until temperature reaches above melting temperature or glass-transition temperature (Lendlein and Kelch, 2002). There are two types of SMPs, which are SMP's based on

melting transition ( $T_M$ ) and SMP's based on glass transition ( $T_g$ ).  $T_M$ -based polymers are often with higher stiffness and faster shape recovery due to presence of "soft-phase" present in general structure of SMP's, such as polyolefin, polyether and polyester. These soft phases possess a low melting temperature which will lead to faster shape recovery and higher switching temperatures due to better crystallization of soft block (Meng and Li, 2013).

Despite many efforts in the development of SMP's, elastomers based SMPs are not common due to their low glass transition temperature which hinder them to perform at ambient temperature environment (Zhang et al., 2009a,b; Koerner et al., 2004). Nevertheless, natural rubber is one of the most commonly known examples for  $T_M$ -based SMPs. It crystallizes when it is strained, which imparts outstanding green strength and tack, and gives natural rubber high resistance to crack growth at severe deformation. The major benefits of shape memory natural rubber (SMNR) lie in its ability to store large strain, mechanical energy and even cold (Heuwers et al., 2013), mechanical and chemical triggering, discrete trigger range (Quitmann et al., 2015), tunable trigger temperature during and after programming (Quitmann et al., 2015; Heuwers et al., 2012), cold programmability and solvent vapor sensitivity (Quitmann et al., 2013, 2014).

Two strategies have been developed to induce the shape memory effect on natural rubber, firstly strain-induced crystallization in weakly cross-linked (0.2%) natural rubber and was firstly reported by Katzenberg et al. (2011). The second method is based upon blending of natural rubber with additives such as fatty acids (Brostowitz et al., 2014). Contrarily,  $T_g$ -based polymers are polymers with glass transition temperature above room temperature.

\* Corresponding author.

E-mail address: [AiBao.Chai@nottingham.edu.my](mailto:AiBao.Chai@nottingham.edu.my) (A.B. Chai).  
Peer review under responsibility of King Saud University.

Production and hosting by Elsevier

Different cross-linking chemistries and densities lead to its properties of having slower shape recovery due to broader glass transition. Due to highly programming and tunability of switching temperature of SMPs, SMPs have been used in several applications which include heat shrinkable polymer tubing (Huang et al., 2005), safety tag (Guangzhou Manborui Material Technology Co. Ltd, 2014), morphing systems, smart Mandrels (Smart Tooling, 2014) etc. An interesting application would be in the field of biomedical engineering as SMPs are very responsive to human senses, tissues and their biodegradability (Small et al., 2010). Metzger et al. conveyed a SMP through a catheter and initiated it photo thermally, which results in a simple expulsion of the coagulation, lastly diminish of the ischemia (Metzger et al., 2002).

Swelling basically involves diffusion of relatively small, mobile molecules into chain segments of a system, such as natural rubber. Liquid molecules diffuse into the rubber just below the surface and eventually into bulk of rubber. As this process proceeds, the rubber will increase in dimensions until concentration of liquid is uniform throughout the rubber component which indicates that equilibrium swelling is achieved (Blow and Hepburn, 1982). Commodity polydiene elastomer, especially natural rubber (NR), cis-polybutadiene (PB) and styrene-butadiene rubber (SBR) are gaining much attraction from the research industries for this SMPs purposes. They are cheap, have good mechanical properties, good elasticity and can be easily cross-linked with additives (Statistics, 1991). Another option is to mix the elastomer with fatty acid or wax as they are low molecular mass organic compound. This would result in crystalline and percolating network in the network of SMP (Brostowitz et al., 2014; Meng and Hu, 2009). There are several experiments and researches that are related to swelling (Brostowitz et al., 2014). Weiss et al. demonstrated addition of fatty acids to ionomers, for example sulfonated ethylene propylene diene monomer (Weiss et al., 2008) where it produces powerful SMPs with high recovery and fixity. Similarly, Huang et al. fabricated shape memory elastomers from mixture of silicone rubber loaded with paraffin wax exhibited two-way, double and triple shape memory properties (Huang et al., 2010). Yet, as reported in Brostowitz et al. (2014), the drawback is that the SMP produced is having relatively poor fixity (<90%) unless the wax loading is high enough and experiences low compressive strains. Lastly, Brostowitz et al. proposed a simple fabrication of SMP using a sulfur cross linked filled rubber band by swelling it in molten stearic acid to create shape fixing temporary network (Brostowitz et al., 2014). Thus, a motivation of this work is to explore the possibility of using palmitic acid as the swelling agent in the fabrication process and investigate the thermomechanical responses of the SMNR.

Palmitic acid is one of the most widely recognized fatty acid found in animals, plants and microorganism (Gunstone et al., 2007). Its chemical formula is  $\text{CH}_3(\text{CH}_2)_{14}\text{CO}_2\text{H}$ . Palmitic acid could act as a retarder as well to retard the onset of curing and vulcanization of rubber (Kirk-Othmer, 1997). According to Morrison and Porter, palmitic acid could be one of the factors contributed to increment of cross-linking density in rubber, which leads to higher tensile strength. But after optimum level (i.e. in excess of 3 phr), softening effect of acid overtook the cross-linking effect and tensile strength reduced (Morrison and Porter, 1984). Even though stearic acid is more widely known to be the swelling agent for rubber, but based on the previous work and researches discussed above, palmitic acid could be a potential candidate for alternative swelling agent. Note that the previous works only studied the experimental characterization of shape memory effects such as shape fixity and recovery efficiencies. In addition, the use of palmitic acid to fabricate SMPs has not been reported yet.

## 2. Material and methods

### 2.1. Materials

Different filler loading of natural rubber samples are purchased from Malaysian Rubber Board. The natural rubber samples consists of standard Malaysian natural rubber grade L as the rubber matrix, different filler loadings of 0, 2 and 5 phr of the Fast Extrusion Furnace (FEF) carbon black-N550 was used. Other compounding ingredients are Zinc oxide, stearic acid, Permax 1,2-dihydro-2,2,4-trimethyl quinoline, N-cyclohexyl-2-benzothiazole sulphonamide, and sulphur. Palmitic acid (Sigma-Aldrich 95%) and Toluene are obtained from the institution's chemical store.

### 2.2. Fabrication of shape memory natural rubber (SMNR)

Natural rubber is cut into strips with desired dimensions and size, which is 3 cm × 1 cm × 0.2 cm. 3 strips of natural rubber samples (0 phr carbon black loading) are immersed into a beaker of molten palmitic acid at 75 °C for 1 h. The swelling experiment is done in water bath of 75 °C, mainly because as temperature increases, the mobility of long chain rubber molecules increases. The rubber becomes softer as the glass transition temperature of rubber is usually small (Gopakumar and Nair, 2005). In addition, since the melting point of palmitic acid is 62.9 °C (Inc. et al., 2005), 75 °C can be considered as the ideal temperature for maximum diffusion of palmitic acid into the gaps between the rubber molecules. For every 10 min, the swollen samples are taken out and the excess liquid on the rubber surface is removed using filter paper. The swollen weight of the rubber samples is measured using digital weighing scale immediately and average value is calculated. After that, three swollen samples are quenched in beaker of 10 °C water. Next, another 3 strips of natural rubber samples (0 phr carbon black loading) are swollen in toluene and average value is obtained. The difference of percentage of mass change in palmitic acid and toluene is then compared to determine equilibrium swelling. Eq. (1) is used to calculate the swelling percentage or weight change percentage:

$$\frac{W_s - W_d}{W_d} \times 100\% \quad (1)$$

where  $W_s$  is the swollen weight and  $W_d$  is the initial dry weight of the rubber samples.

The whole process is then repeated for 2 phr and 5 phr natural rubber.

### 2.3. Characterization

#### 2.3.1. Determination of cross-link density

To determine if equilibrium swelling is achieved by palmitic acid in rubber samples, cross-link density is determined by swelling rubber samples in palmitic acid at room temperature as detailed in Section 2.2. The cross-link density obtained is then compared with the results obtained from the rubber samples swollen in toluene. The volume fraction of the rubber samples was calculated using Eq. (2):

$$v_r = \frac{1}{1 + \frac{\rho_r}{\rho_s} \left( \frac{W_s - W_d}{W_d} \right)} \quad (2)$$

where  $\rho_r$  is the density of the rubber,  $\rho_s$  is the density of the solvent. The effective crosslink density of the natural rubber can then be determined using the Flory-Rehner equation (Flory and Rehner, 1943):

$$-\ln(1 - v_r) + v_r + Xv_r^2 = V_s n \left( v_r^{\frac{1}{2}} - \frac{v_r}{2} \right) \quad (3)$$

where  $V_s$  is the molar volume of the solvent,  $X$  is the Flory Huggins interaction parameter and  $n$  is the effective cross-link density of the swollen rubber. The Flory Huggins interaction parameter was calculated using equation based on Hansen solubility parameters,  $\delta_1$  for palmitic acid and  $\delta_2$  for rubber (Hansen, 2013):

$$X = \frac{V_s}{RT(\delta_1 - \delta_2)^2} \quad (4)$$

### 2.3.2. Shape memory testing

Brostowitz et al. (2014) proposed a method to measure the shape memory behavior and this is adopted in the current work. An adjustable spanner is modified to test the shape memory behavior of the swollen rubber samples under uniaxial tension, shown schematically in Fig. 1. A 12", 34 mm adjustable spanner is used along with two mini clamps to secure a 3 cm × 1 cm × 0.2 cm strip of swollen rubber sample. The adjustable spanner also comes with clear and accurate scale on top of it for better measurement of repeatable elongations. Overall, this adjustable spanner is the perfect tool to demonstrate shape memory testing of the rubber samples due to rapid temperature changes when immersing the rubber samples into the water baths. For the shape memory testing, the swollen rubber sample (0 phr carbon black loading) is clamped on the adjustable spanner using two mini clamps. Gauge length of the initial rubber sample,  $l_i$  is marked with a pen and measured with callipers. Next, the swollen rubber sample is immersed in a 75 °C water bath for 15 s, stretched to 100% strain and the stretched length,  $l_s$  is measured using callipers. Immediately, the rubber sample is quenched in a 10 °C of ice water bath for 15 s, the stretched rubber sample is then removed from the spanner and the fixed length,  $l_f$  is measured. Lastly, the fixed length rubber is immersed back to the 75 °C water bath again for another 15 s, quench in 10 °C of ice water bath for 15 s and the recovery length,  $l_r$  is measured with callipers. After

all the data is collected, shape fixity ( $F$ ) and shape recovery ( $R$ ) efficiencies of the swollen rubber sample is calculated using Eqs. (5) and (6):

$$F = \frac{\varepsilon_f}{\varepsilon_s} \times 100\%, \quad (5)$$

$$R = \frac{\varepsilon_f - \varepsilon_r}{\varepsilon_f - \varepsilon_i} \times 100\%, \quad (6)$$

where  $\varepsilon_f$  is the change in fixed length,  $\varepsilon_s$  is the change in stretched length,  $\varepsilon_r$  is the change in recovery length and  $\varepsilon_i$  is the change in initial gauge length. The whole process is then repeated for 2 phr and 5 phr natural rubber.

### 2.3.3. Repeatability and reproducibility testing

New SMNR samples are fabricated and tested under the same manual, strain deformation over 3 cycles (3 days). The fixity and recovery efficiencies under 100%, 150% and 200% strain are then recorded. To find out whether the shape memory properties could be restored, the used SMNR samples are re-swollen with palmitic acid for 1 h and re-tested under the same manual strain deformation. The fixity and recovery efficiencies are then recorded and compared with the value before re-swelling process.

### 2.3.4. Dynamic mechanical analysis (DMA)

For this analysis, dynamic mechanical analysis instrument (Perkin Elmer DMA8000) is used. DMA is a mechanical test which is controlled by force with an enclosed temperature chamber that is most applicable for testing the inherent thermal viscoelastic responses of polymer (Osswald and Menges, 2012). The natural rubber samples used for testing are 3 cm × 1 cm with a gauge length of 1 cm. Temperature ramps of 10 °C/min is used. Firstly, the natural rubber samples underwent preheating to allow the creep to reach equilibrium, giving more precise measurement of shape memory properties. In this work, the procedures proposed by Brostowitz et al. (2014) is adopted. The preheat cycle is: ramp to 75 °C, isothermal hold for 10 min, ramp to 30 °C, and isothermal

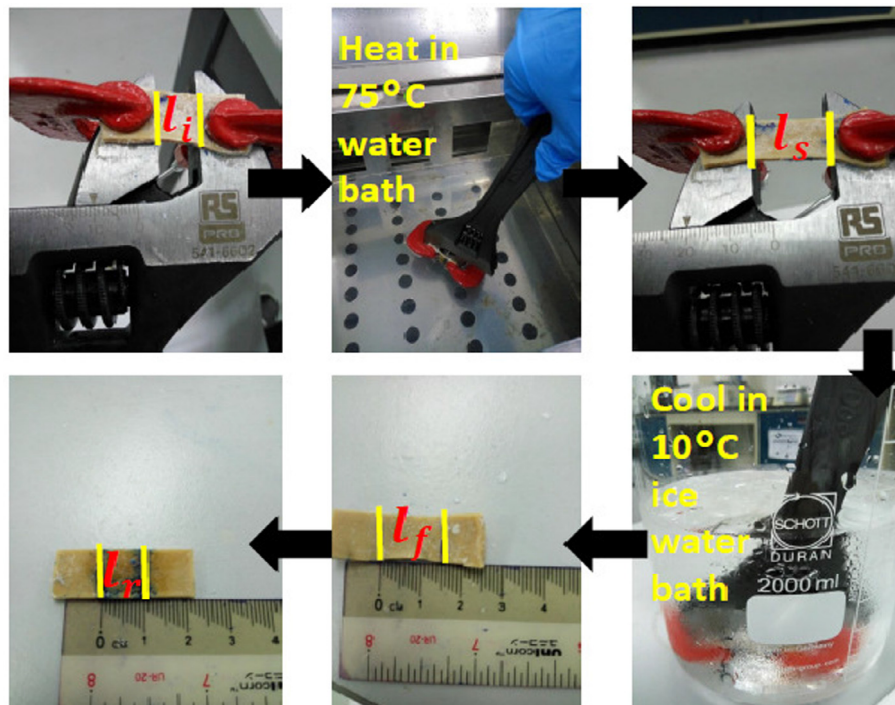


Fig. 1. Shape memory cycle tested with adjustable spanner and mini clamps.

hold for 10 min. Next, the shape fixing cycle is: ramp to 75 °C, hold for 5 min isothermally, ramp force at 3 mm/N, ramp to 30 °C, hold for another 5 min at the same temperature, step force to 0.00 mm/N and isothermal hold for 5 min again. Lastly, shape recovery cycle is tested by: ramp to 75 °C, isothermal hold for 10 min, ramp to 30 °C, and isothermal hold for 10 min.

### 2.3.5. Scanning electronic microscopy

The FEI QUANTA 400F scanning electron microscope (SEM) is used to obtain micrographs of the SMNR samples produced. Small samples from the SMNR are cut with a sharp blade and the morphological properties of the sample are observed. The power used is 10 kv, magnification of 2500 $\times$ , at a working distance of 8.4 mm. The surfaces of the samples are covered with thin layers of palladium, Pd, to prevent electron charging of the samples during the experiment.

## 3. Results and discussions

### 3.1. Degree of swelling of natural rubber in palmitic acid and toluene

The diffusion mechanism is closely related to the ability of the rubber to provide pathways for the solvent uptake into the network chain. In this experiment, different carbon black loading of rubber is used and thus different swelling percentage (weight change percentage) can be observed.

Fig. 2 shows the weight change percentage of natural rubber samples with different carbon black loadings. The weight change percentage for 0 phr is the highest, 31.20%, followed by 2 phr and 5 phr, which are 22.46% and 18.70% respectively. As carbon black loading increases, equilibrium palmitic acid uptake decreases. Carbon black could act as a barrier to limit the solvent from penetrating into the natural rubber molecules (Sheng et al., 1996).

Since there is a better bonding between carbon black filler and rubber, a strong interface is established, which control the entry of solvent. Thus, at higher carbon black loadings, extra hindrances exerted by the filler causes decrease in the swelling percentage of rubber (Jacob et al., 2004). Furthermore, it can be seen that all three rubber's weight change percentages reach a plateau region at approximately 50 min. This is the time where the maximum uptake of palmitic acid takes place. Same phenomenon is observed for the samples swollen in toluene where 0 phr has the highest weight change percentage, followed by 2 phr and 5 phr.

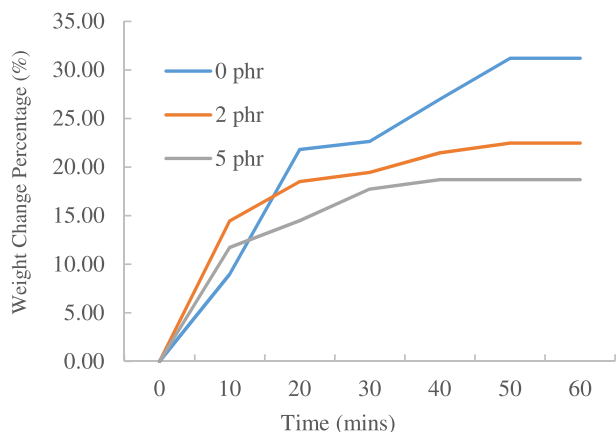


Fig. 2. Graph of weight change percentage of natural rubber samples against time swollen in palmitic acid.

### 3.2. Effective cross-link density of natural rubber

Cross-link density of 0 phr rubber sample is first calculated. Table 1 shows the material constants used for this purpose.  $X$  of  $1.296E-6$  at 75 °C is obtained based on the Hansen solubility parameters of palmitic acid ( $\delta_1 = 17.86 \text{ MPa}^{1/2}$ ) and natural rubber ( $\delta_2 = 17.55 \text{ MPa}^{1/2}$ ). Using swelling data of palmitic acid,  $v_r$  is calculated as  $0.72 \pm 0.03$ , which leads to an effective cross-link density,  $n$  of  $0.0036 \text{ mmol/cm}^3 \pm 0.0014$ . For toluene, an average cross-link density of  $0.001 \text{ mmol/cm}^3 \pm 0.001$  is obtained.

The similarity between the effective cross-link density of palmitic acid, toluene and stearic acid (Brostowitz et al., 2014) indicates that the swelling condition could achieve equilibrium concentrations of palmitic acid in the rubber samples. For 2 phr and 5 phr, the effective cross-link density of natural rubber is calculated to be 0.0045 and 0.0049 mmol/cm<sup>3</sup> respectively. It is noted that 5 phr has the highest cross-link density and 0 phr has the lowest. In practice, the density of crosslinking in rubber increases proportionally with increasing carbon black loadings, resulting with rise of network elasticity contributions (Kader and Bhowmick, 2003). The cross-linkages formed restrict extensibility of rubber chains induced by swelling and make it harder for palmitic acid and toluene to diffuse into the gap between rubber molecules. Hence, the swelling percentages drop and counter the tendency for dissolution. This proves that the data in Section 3.1 is valid where swelling reduces with increase of cross-linking network.

### 3.3. Shape fixity and recovery efficiencies of natural rubber

Figs. 3 and 4 show the shape fixity efficiencies and shape recovery efficiencies of natural rubber with different carbon black loadings. Results showed that the natural rubber samples exhibited averagely excellent shape memory properties under 100% strain. This indicates that procedures proposed by Brostowitz et al. (2014) are applicable to palmitic acid as well where there were rapid melting or crystallization of the palmitic acid under the selected temperatures and immersion times. Also, the modified wrench provided consistent strain control over multiple cycles and between samples.

At 100% strain, the fixity efficiency for 3 rubber samples of 0 phr was 80%, while 66.67% and 56.67% for 2 phr and 5 phr rubber samples respectively. As for recovery efficiency, 3 rubber samples of 0 phr showed an average of 83.33% of recovery rate, followed by 83.07% and 68% for 2 phr and 5 phr.

These shape memory properties are induced by the melting or forming of the palmitic acid crystallized network and entropic recovery force of the cross-link natural rubber (Brostowitz et al., 2014). Since rubber samples with 5 phr carbon black loading has the least amount of palmitic acid diffused into the rubber molecules, they are expected to have the lowest fixity and recovery efficiencies which are proven in the results collected in Figs. 3 and 4. Another reason to explain this phenomenon is that as carbon content increases, there could be more rapid rubber-filler interactions which cause the increase in hardness and tensile strength (Saad and Sh Fayed, 0000). Carbon black is then able to impart greater

Table 1  
Material constants for palmitic acid, toluene and stearic acid used to calculate cross-link density.

|  | Palmitic Acid | Toluene | Stearic Acid (Brostowitz et al., 2014) |
|--|---------------|---------|--|
| Density, $\rho$ (g/cm <sup>3</sup> )       | 0.852         | 0.867   | 0.941                                  |
| Molar volume, $V_s$ (cm <sup>3</sup> /mol) | 300.96        | 106.83  | 652                                    |
| $\delta_1$ (MPa <sup>1/2</sup> )           | 17.86         | 18.2    | 17.52                                  |
| $n$ (mmol/cm <sup>3</sup> )                | 0.0036        | 0.001   | 0.0028                                 |

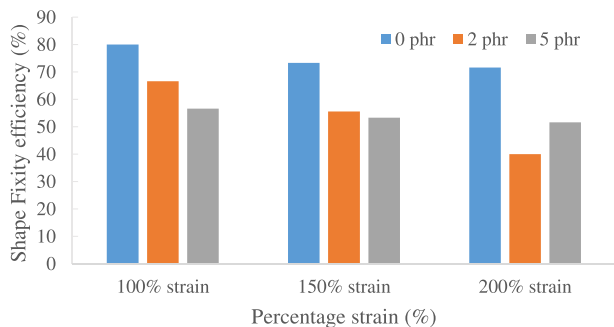


Fig. 3. Bar chart of shape fixity efficiencies of natural rubber.

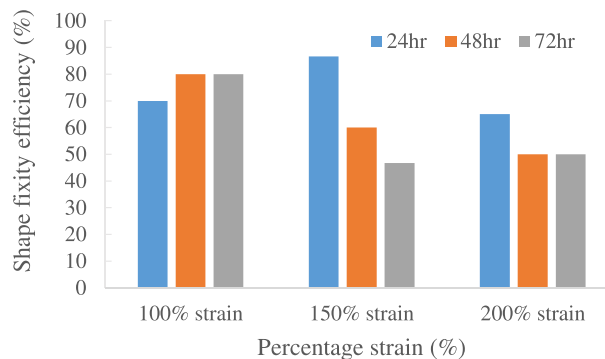


Fig. 5. Repeatability of shape fixity efficiencies of natural rubber (0 phr) in 72 h.

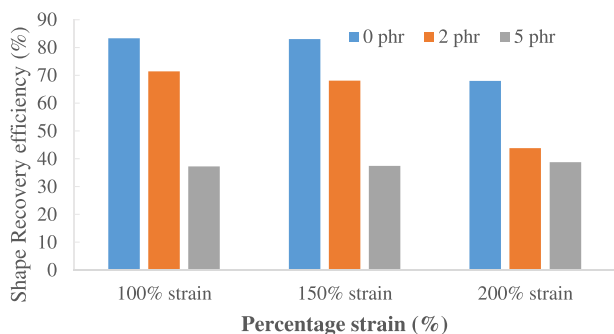


Fig. 4. Bar chart of shape recovery efficiencies of natural rubber.

stiffness to the filled vulcanizates, reducing the mobility of the rubber chains (Ismail et al., 2001). Consequently, the rubber sample loses its elasticity and hence reducing its efficiency in shape fixing and recovery. Therefore, even though rubber with higher carbon content has higher strength, the drawback is that they will have weaker shape memory properties. Next, to test the endurance of the shape memory natural rubber, 150% strain and 200% strain tests were applied to the rubber samples. Results showed that, with higher strain used, the shape fixity and recovery efficiency decreased drastically. This can be explained by the fact that as higher strain is applied, the elongation at break of the rubber decreases. It expresses the ability of the rubber to resist alteration of shape without crack formation is no longer as good as 100% strain. When 200% strain was used, crack was observed to form at the rubber surface.

3.4. Repeatability and reproducibility of the shape memory natural rubber

To study the repeatability and reproducibility, shape memory cycles of SMNR should be tested more than once. According to Matsumoto et al. (2012), the electro spun non-woven shape memory fibres demonstrated excellent thermomechanical repeatability over three cycles. Hence, for this experiment, another three new shape memory natural rubber samples (0 phr) were fabricated and tested for 3 cycles. The reason only 0 phr rubber samples were refabricated is because rubber samples of 0 phr showed better shape memory properties compared to 2 phr and 5 phr as described in Section 3.3.

Fig. 5 shows the repeatability of shape fixity efficiencies of natural rubber in 72 h. Under 100% strain, the rubber sample showed a 70% of fixity efficiency on first cycle, while on second cycle it deduced to 80%. However, the shape fixity stayed constant at 80% over the third cycle. Even though the repeatability of shape

recovery (Fig. 6) showed a decreasing trend, these results suggested that the 0 phr shape memory natural rubber enjoyed favourable repeatability shape memory properties under 100% strain. On the other hands, the repeatability result shown in 150% and 200% strain was not as convincing as they only had decreasing trend both in fixity and recovery over 3 cycles. One reason to explain this is because the shape memory natural rubber has reached fatigue failure (Mammano and Dragoni, 2011) as crack started to form at 200% strain due to constant strain-test over 3 cycles. The SMNR loses its stiffness and thus cannot remember its original shape well enough, resulting with decrease in shape fixity and recovery rate. Thus, under 150% and 200% strain, the maximum cycle-life that the natural rubber could withstand is only 1 cycle before a noticeable decrease in shape fixity and recovery is observed (Kong and Xiao, 2016). This further supports that the SMNR samples fabricated are not suitable to be stretched with 150% strain and above. With that, it is safe to assume that 100% strain is the more desirable strain for shape memory properties.

Taking 100% strain as reference, a re-swelling experiment was conducted to test the reproducibility of the SMNR. As seen in Fig. 7, at the first 24 h, the shape fixity efficiency improved from 70% to 80% after re-swelling. This shows that the SMNR has ability to be reproduced after re-swollen with palmitic acid. At 36 and 72 h, it stayed constant for 80% which also proved its repeatability over three cycles. While, for shape recovery efficiency (Fig. 8), the value after re-swelling was lower than the original value but it stayed the same over the third cycle, which was around 50%.

Therefore, it is believed that the SMNR has an average of 50% recovery efficiency over 3 cycles. With that, the SMNR fabricated is verified to have satisfactory repeatability, reusability and reproducibility.

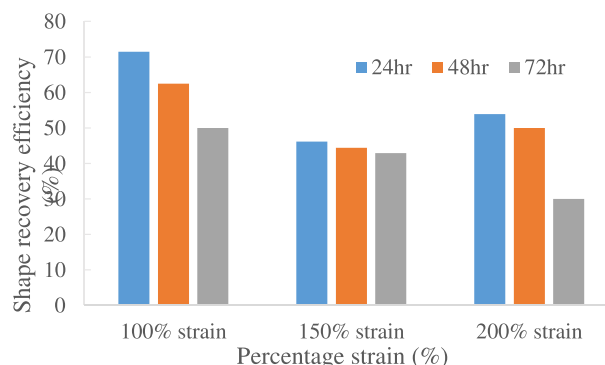


Fig. 6. Repeatability of shape recovery efficiencies of natural rubber (0 phr) in 72 h.

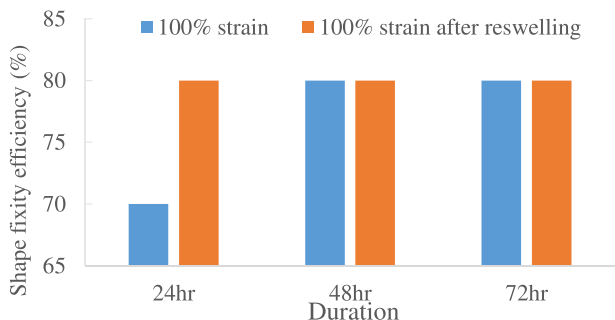


Fig. 7. Repeatability of shape fixity efficiency of 0 phr natural rubber in 72 h after re-swelling.

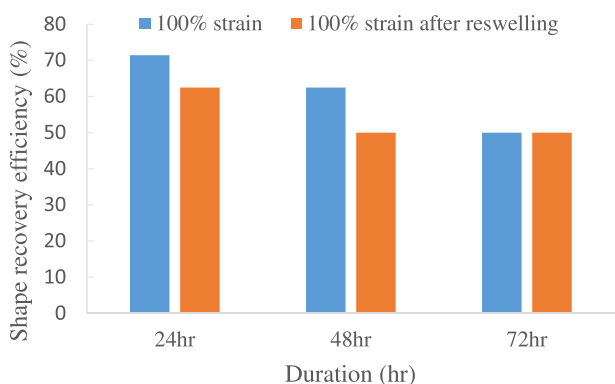


Fig. 8. Repeatability of shape recovery efficiency of 0 phr natural rubber in 72 h after re-swelling.

3.5. Dynamic mechanical analysis (DMA) results

The deformation method of the DMA machine (Perkin Elmer 8000) is set to be in tension geometry. In tension geometry, the sample is being pulled which is most useful for thin films, such as rubber samples. To ensure the natural rubber samples remain stiff, the clamp has to be constantly calibrated and adjusted for every new sample tested. As suggested in Brostowitz et al. (2014), before conducting the shape memory cycle test, pre-heating/cooling was applied so as to reduce the creep effect in the sample during testing. This is because at higher temperature, there is constant force applied by the clamp. After calibrating and adjusting of the clamp, it was found that a significant downward force was applied to the natural rubber sample even when

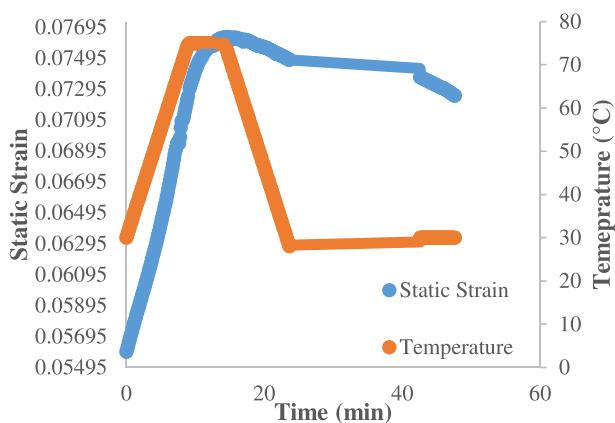


Fig. 9. DMA preheating cycle.

there was no applied tension force. As shown in Fig. 9, a creep of 0.07493 occurred when holding the sample at 30 °C at around 10 min. Due to the preheating of the sample, the creep remained relatively stable thereafter before the shape memory cycle started. The sample was then heated above the melting temperature of palmitic acid to 75 °C, held for 10 min, and then cooled back to ‘activate’ the shape memory properties. These observations tally with the phenomenon reported by Brostowitz et al. (2014).

The shape memory cycle started right after the preheating cycle. Due to the DMA machine model limitations, preheating and shape memory cycle testing has to be done separately, thus a combined strain vs time graph could not be obtained. Besides that, the tension applied can only be set to maximum 3 mm/N due to the limitation of the machine. Thus, the static strain value obtained was recorded to be as low as 0.07.

As shown in Fig. 10, all three natural rubber samples with different carbon black loading exhibited different shape memory properties. Fixity could be seen at around 10–20 min, while recovery could be seen at 0–10 min and 20–30 min. Based on the DMA data, calculation of shape fixity and recovery efficiency can be done in Table 2.

It is observed that 0 phr natural rubber has the highest shape fixity efficiency, 99.5% and the highest shape recovery efficiency, 97.36%, followed by 2 phr and 5 phr. These fixity and recovery efficiencies are comparatively very much higher than the ones in Section 3.3 due to the relatively low tension force (3 mm/N) used in DMA testing. But, both the manual strain-controlled and DMA result showed similar trend, where 0 phr has the best shape fixity and recovery efficiency as maximum amount of palmitic acid were swollen inside the natural rubber network. This observation is consistent with the results presented in Section 3.3. For DMA testing, the recovery is generally lower than the fixity because of the constant tensile force of the clamp. It will both increase the creep of the sample during shape recovery and inhibit the elastic recovery, which is driven by entropic restoring force of the crystal network in the natural rubber (Brostowitz et al., 2014).

3.6. SEM micrographs

Palmitic acid, similar to steric acid is a type of fatty acids that grow as crystal platelets via forming of bilayers and fatty acids are known to gel vegetable oils (Schaink et al., 2007). The palmitic acid crystals were observed to form a continuous network and the platelet formation could be seen on the crystallization front as shown in the Fig. 11. In Fig. 11, there are more palmitic acid crystals formed on the surface of the 0 phr natural rubber sample compared to 2 phr and 5 phr. This is once again due to 0 phr natural

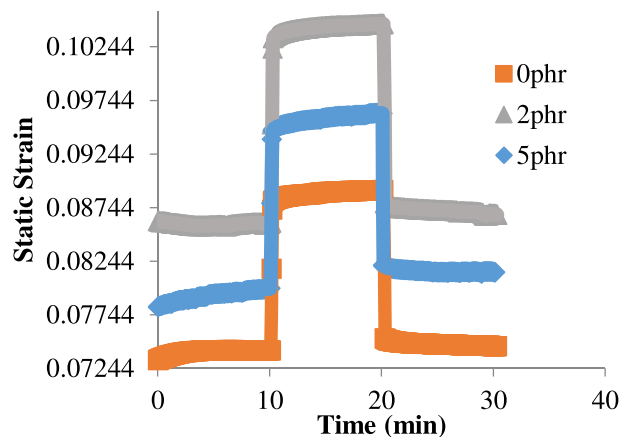
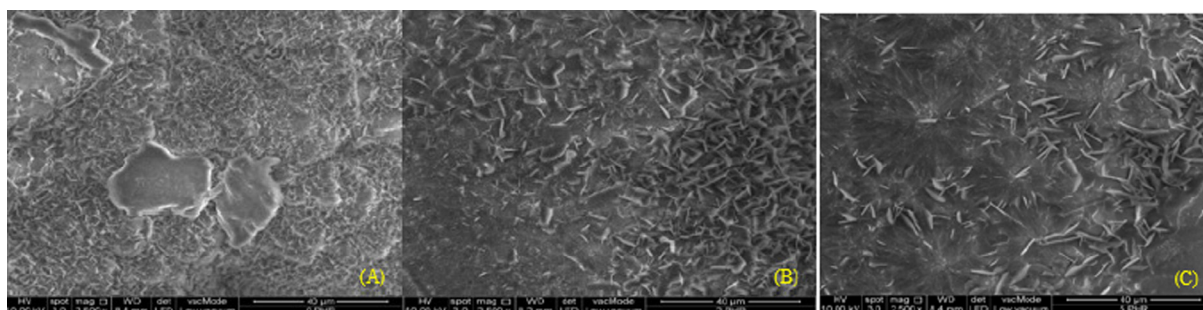


Fig. 10. DMA shape memory cycle.

**Table 2**

Compilation of DMA shape memory data versus time.

|                               | Time (min) | 0 phr    | 2 phr    | 5 phr    |
|-------------------------------|------------|----------|----------|----------|
| $\epsilon_i$                  | 5          | 0.072504 | 0.084722 | 0.07763  |
| $\epsilon_s$                  | 10         | 0.074147 | 0.085781 | 0.079393 |
| $\epsilon_f$                  | 17         | 0.088561 | 0.103979 | 0.095343 |
| $\epsilon_r$                  | 23         | 0.089026 | 0.104473 | 0.096082 |
|                               | 38         | 0.074794 | 0.087327 | 0.081559 |
|                               | 45         | 0.074539 | 0.08677  | 0.081433 |
| Shape fixity efficiency (%)   |            | 99.47768 | 99.52677 | 99.23128 |
| Shape recovery efficiency (%) |            | 97.36376 | 94.70917 | 87.77831 |



**Fig. 11.** SEM images of crystallized palmitic acid formed on the surface of natural rubber with (A) 0 phr, (B) 2 phr, (C) 5 phr carbon black loading. All samples are viewed with the power of 10 kv, magnification of 2500 $\times$ , at a working distance of 8.4 mm with the same resolution of 40  $\mu$ m for the ease of comparison.

rubber sample has maximum allowance for the swelling of palmitic acid into the space between rubber molecules.

#### 4. Conclusions

The present work shows that palmitic acid could be a good swelling agent to induce shape memory properties to natural rubber. It is found that the shape fixity and recovery efficiency vary with different carbon black loading. Under manual, strain-controlled tensile deformation, 0 phr natural rubber shows the best shape fixity and recovery of 80%  $\pm$  10%, followed by 2 phr and 5 phr. Yet the efficiency drops as the percentage of strain increases, especially when crack starts to form at 200% strain. Moreover, it is discovered that the SMNR shows satisfactory repeatability and reproducibility over 3 cycles of time, 24-h, 48-h and 72-h. In DMA analysis, the natural rubber samples have similar shape fixity and recovery trend compared to the manual strain controlled tensile test. Lastly, thermal, microscopic studies proved that palmitic acid forms crystal networks within the natural rubber. These networks are the main drivers for inducing thermal shape memory properties, where deformation and recovery could occur above the melting point of palmitic acid, and fixation below that point (Brostowitz et al., 2014).

Further works are proposed to monitor the trigger temperature and recovery temperature to improve the efficiency and recovery ratio of the palmitic acid based SMNR. Further research on shape memory rubber should be expanded to other elastomeric polymers and fatty acid. Also, thermal gravimetric analysis (TGA) analysis could be done to examine the fatty acid loading in the elastomer.

#### References

Blow, C.M., Hepburn, C., 1982. Rubber Technology and Manufacture. Butterworths Scientific, London.

Brostowitz, N.R., Weiss, R.A., Cavicchi, K.A., 2014. Facile fabrication of a shape memory polymer by swelling cross-linked natural rubber with stearic acid. ACS Macro. Lett. 3 (4), 374–377.

Feil, H., Bae, Y.H., Feijen, J., Kim, S.W., 1992. Mutual influence of Ph and temperature on the swelling of ionizable and thermosensitive hydrogels. Macromolecules 25 (20), 5528–5530.

Flory, P.J., Rehner, J., 1943. Statistical mechanics of cross-linked polymer networks I Rubberlike elasticity. J. Chem. Phys. 11 (11), 512–520.

Gopakumar, S., Nair, M.R.G., 2005. Swelling characteristics of NR/PU block copolymers and the effect of NCO/OH ratio on swelling behaviour. Polymer 46 (23), 10419–10430.

Gunstone, F.D., Harwood, J.L., Dijkstra, A.J., 2007. The lipid handbook. CRC Press, London.

Hansen, C.M., 2013. Hansen Solubility Parameters A User's Handbook.

Heuwers, B., Quitmann, D., Katzenberg, F., Tiller, J.C., 2012. Stress-induced melting of crystals in natural rubber: a new way to tailor the transition temperature of shape memory polymers. Macromol. Rapid. Comm. 33 (18), 1517–1522.

Heuwers, B., Beckel, A., Krieger, A., Katzenberg, F., Tiller, J.C., 2013. Shape-memory natural rubber: an exceptional material for strain and energy storage. Macromol. Chem. Phys. 214 (8), 912–923.

Hu, J.L., Zhu, Y., Huang, H.H., Lu, J., 2012. Recent advances in shape-memory polymers: structure, mechanism, functionality, modeling and applications. Prog. Polym. Sci. 37 (12), 1720–1763.

Huang, W.M., Yang, B., An, L., Li, C., Chan, Y.S., 2005a. Water-driven programmable polyurethane shape memory polymer: demonstration and mechanism. Appl. Phys. Lett. 86 (11), 1–3.

Huang, W.M., Yang, B., An, L., Li, C., Chan, Y.S., 2005b. Water-driven programmable polyurethane shape memory polymer: demonstration and mechanism. Appl. Phys. Lett. 86 (11), 1–3.

Huang, W.M., Ding, Z., Wang, C.C., Wei, J., Zhao, Y., Purnawali, H., 2010. Shape memory materials. Mater. Today 13 (7–8), 54–61.

Inc., S.c., 2005. Material Safety Data Sheet Hydrochloric acid MSDS. vol. 3, pp. 1–7.

Ismail, H., Nizam, J.M., Khalil, H.P.S.A., 2001. The effect of a compatibilizer on the mechanical properties and mass swell of white rice husk ash filled natural rubber/linear low density polyethylene blends. Polym. Test. 20 (2), 125–133.

Jacob, M., Thomas, S., Varughese, K.T., 2004. Mechanical properties of sisal/oil palm hybrid fiber reinforced natural rubber composites. Compos. Sci. Technol. 64 (7–8), 955–965.

Kader, M.A., Bhowmick, A.K., 2003. Rheological and viscoelastic properties of multiphase acrylic rubber/fluoroelastomer/polyacrylate blends. Polym. Eng. Sci. 43 (4), 975–986.

Katzenberg, F., Heuwers, B., Tiller, J.C., 2011. Superheated rubber for cold storage. Adv. Mater. 23 (16), 1909–1911.

Kirk-Othmer, 1997. Kirk-Othmer Encyclopedia of Chemical-Technology. Kirk-Othmer Encyclopedia of Chemical-Technology 24, 233–250.

Koerner, H., Price, G., Pearce, N.A., Alexander, M., Vaia, R.A., 2004. Remotely actuated polymer nanocomposites – stress-recovery of carbon-nanotube-filled thermoplastic elastomers. Nat. Mater. 3 (2), 115–120.

Kong, D.Y., Xiao, X.L., 2016. High cycle-life shape memory polymer at high temperature. Sci. Rep.-Uk 6.

Lee, K.M., Koerner, H., Vaia, R.A., Bunning, T.J., White, T.J., 2011. Light-activated shape memory of glassy, azobenzene liquid crystalline polymer networks. Soft Matter. 7 (9), 4318–4324.

- Lendlein, A., Kelch, S., 2002. Shape-memory polymers. *Angew. Chem. Int. Ed.* 41 (12), 2034–2057.
- Luo, H.S., Li, Z.W., Yi, G.B., Wang, Y.J., Zu, X.H., Wang, H., Huang, H.L., Liang, Z.F., 2015. Temperature sensing of conductive shape memory polymer composites. *Mater Lett.* 140, 71–74.
- Mammano, G.S., Dragoni, E., 2011. Functional fatigue of shape memory wires under constant-stress and constant-strain loading conditions. *Proc. Eng.* 10, 3692–3707.
- Matsumoto, H., Ishiguro, T., Konosu, Y., Minagawa, M., Tanioka, A., Richau, K., Kratz, K., Lendlein, A., 2012. Shape-memory properties of electrospun non-woven fabrics prepared from degradable polyesterurethanes containing poly (omega-pentadecalactone) hard segments. *Eur. Polym. J.* 48 (11), 1866–1874.
- Meng, Q.H., Hu, J.L., 2009. A review of shape memory polymer composites and blends. *Compos. Part A-Appl. S.* 40 (11), 1661–1672.
- Meng, H., Li, G.Q., 2013. A review of stimuli-responsive shape memory polymer composites. *Polymer* 54 (9), 2199–2221.
- Metzger, M.F., Wilson, T.S., Schumann, D., Matthews, D.L., Maitland, D.J., 2002. Mechanical properties of mechanical actuator for treating ischemic stroke. *Biomed. Microdev.* 4 (2), 89–96.
- Morrison, N.J., Porter, M., 1984. Temperature effects on the stability of intermediates and crosslinks in sulfur vulcanization. *Rubber. Chem. Technol.* 57 (1), 63–85.
- Osswald, T.A., Menges, G., 2012. *Materials science of polymers for engineers*, Carl Hanser Verlag GmbH Co KG.
- Quitmann, D., Gushterov, N., Sadowski, G., Katzenberg, F., Tiller, J.C., 2013. Solvent-sensitive reversible stress-response of shape memory natural rubber. *ACS Appl. Mater. Inter.* 5 (9), 3504–3507.
- Quitmann, D., Gushterov, N., Sadowski, G., Katzenberg, F., Tiller, J.C., 2014. Environmental memory of polymer networks under stress. *Adv. Mater.* 26 (21), 3441–3444.
- Quitmann, D., Reinders, F.M., Heuwers, B., Katzenberg, F., Tiller, J.C., 2015. Programming of shape memory natural rubber for near-discrete shape transitions. *ACS Appl. Mater. Inter.* 7 (3), 1486–1490.
- Saad, I.S., Sh Fayed, M., Abdel-Bary, E.M., Effects of Carbon Black Content on Cure Characteristics, Mechanical Properties and Swelling Behaviour of 80/20 NBR/CIIR Blend. 13th International Conference on Aerospace Science and Aviation Technology. 9.
- Schaik, H.M., van Malssen, K.F., Morgado-Alves, S., Kalnin, D., van der Linden, E., 2007. Crystal network for edible oil organogels: possibilities and limitations of the fatty acid and fatty alcohol systems. *Food Res. Int.* 40 (9), 1185–1193.
- Sheng, E., Sutherland, I., Bradley, R.H., Freakley, P.K., 1996. Effects of a multifunctional additive on bound rubber in carbon black and silica filled natural rubbers. *Eur. Polym. J.* 32 (1), 35–41.
- Small, W., Singhal, P., Wilson, T.S., Maitland, D.J., 2010. Biomedical applications of thermally activated shape memory polymers. *J. Mater. Chem.* 20 (17), 3356–3366.
- Statistics, W.R., 1991. *International Institute of Synthetic Rubber Producers Houston*.
- Tsukada, G., Tokuda, M., Torii, M., 2014. Temperature triggered shape memory effect of transpolyisoprene-based polymer. *J. Endodont.* 40 (10), 1658–1662.
- Weiss, R.A., Izzo, E., Mandelbaum, S., 2008. New design of shape memory polymers: mixtures of an elastomeric ionomer and low molar mass fatty acids and their salts. *Macromolecules* 41 (9), 2978–2980.
- Wu, Y.P., Lin, Y.H., Zhou, Y., Zuo, F., Zheng, Z.H., Ding, X.B., 2012. Light-induced shape memory polymer materials. *Prog. Chem.* 24 (10), 2004–2010.
- Guangzhou Manborui Material Technology Co. Ltd, 2014. SMP security label. <https://www.china-mbr.com/security-label>. (Assessed: 23.11.16).
- Smart Tooling, 2014. Smart Mandrels. <http://www.smarttooling.com/products/smart-mandrels>. (Assessed: 23.11.16).
- Zhang, H., Wang, H.T., Zhong, W., Du, Q.G., 2009a. A novel type of shape memory polymer blend and the shape memory mechanism. *Polymer* 50 (6), 1596–1601.
- Zhang, W., Chen, L., Zhang, Y., 2009b. Surprising shape-memory effect of polylactide resulted from toughening by polyamide elastomer. *Polymer* 50 (5), 1311–1315.